# Synthesis and Characterization of a Series of $[M_2(\beta\text{-SiW}_8O_{31})_2]^{n-}$ Clusters and Mechanistic Insight into the Reorganization of {β-SiW$_8$O$_{31}$} into {α-SiW$_9$O$_{34}$}

Ross S. Winter, De-Liang Long, and Leroy Cronin*

School of Chemistry, WestCHEM, University of Glasgow, Glasgow G12 8QQ, U.K.

Ⓢ *Supporting Information*

ABSTRACT: Lacunary polyoxometalates of low nuclearity are difficult to synthesize in isolation. We report the facile synthesis of six {M$_2$(B-β-SiW$_8$O$_{31}$)$_2$} clusters (M = Co/Mn/Ni/Zn/Cu^{2+}, Fe^{3+}) that can be employed as building blocks for the formation of larger architectures. We show for the first time that such {B-β-SiW$_8$O$_{31}$} lacunae are capable of reorganizing into larger Keggin lacunary species even in the absence of an external source of tungstate. We hypothesize, based on electrospray ionization mass spectrometry evidence obtained, not only that such a transformation is only possible via an initial decomposition of the {SiW$_8$} precursor into a {SiW$_6$}-based intermediate but also that it is this {SiW$_6$} species that acts as the template for the growth of the larger fragments.
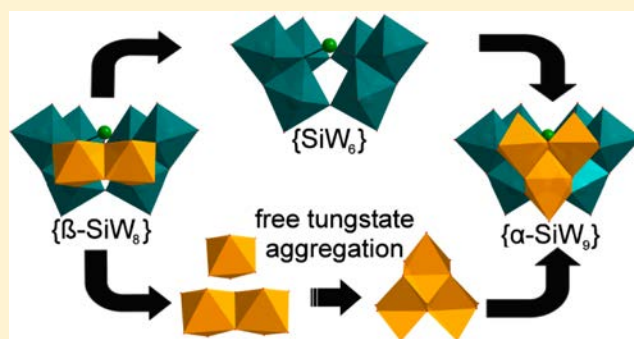
INTRODUCTION

Polyoxometalates (POMs) are a large class of inorganic metal oxide clusters with potential applications across a wide range of areas such as catalysis,[1,2] nanomaterials,[3,4] magnetism,[5,6] and even medicine.[7] A subset of POMs is transition metal substituted POMs (TMSPs), which comprise transition metals coordinated by POM building blocks organized into intricate and complex nanoscale architectures.[8−10] A common way of synthesizing such TMSPs is to use lacunary POMs as precursors. Lacunary POMs possess predefined coordination sites that are primed for reaction with transition metals and enable a degree of control over how the final architecture will self-assemble.[11] However, lacunary POMs have the interesting capacity to reorganize in solution, facilitating the formation of different POM building blocks.[12] This introduces the potential for even more complicated architectures to arise from seemingly simple reaction systems, but this conversely makes prediction and control over TMSP reactions more difficult. The challenge within POM chemistry is to understand how lacunary POM transformations occur and to learn how best to control the reorganization of such dynamic building blocks, via careful tuning of the reaction parameters.

The most versatile lacunary POMs in terms of reorganizational ability are the Keggin-type $[\gamma\text{-XW}_{10}O_{36}]^{8-}$ (X = Ge, Si) clusters,[13] which are known to isomerize into the {α/β-W$_{10}$} species[14,15] and also to respeciate into units of nuclearity {W$_{11}$},[16] {W$_9$},[17−19] {W$_8$},[20−22] and even {W$_6$}.[23] Often final architectures possess more than one type of POM building unit.[24−26] The greater the number of vacancies in a lacunary fragment, the more transition metals can be incorporated into the final architecture, and so there is a need to find reliable ways

of synthesizing smaller lacunary fragments that can be used to generate highly substituted TMSPs. Low-nuclearity lacunary fragments may also be the intermediate architectures formed during lacunary POM reorganization, and if they could be isolated this hypothesis can be investigated.

Herein, we report the formation of a series of $[M_2(B\text{-}\beta\text{-SiW}_8O_{31})_2]^{n-}$ (M = Cu/Co/Mn/Ni/Zn^{2+}, Fe^{3+}; n = 16, 14) TMSPs, making use of the organic additive N,N'-bis(2-hydroxyethyl)-piperazine (BHEP) to control the speciation. Furthermore, the $[Cu_2(SiW_8O_{31})_2]^{16-}$ cluster has been shown to be a valid starting material for the synthesis of other TMSPs, including the well-documented Weakley sandwich cluster $[Cu_4(H_2O)_2(B\text{-}\alpha\text{-SiW}_9O_{34})_2]^{12-}$.[27] This reaction represents a direct transformation of {B-β-SiW$_8$} into {B-α-SiW$_9$} in the absence of any external source of tungstate, meaning that the increase in nuclearity from {W$_8$} to {W$_9$} arises from an initial decomposition of the starting material into a smaller species, which then undergoes reconstitution with the generated free tungstate from said original decomposition. Electrospray ionization mass spectrometry (ESI-MS) analysis of the starting material indicates that this lower-nuclearity fragment is {SiW$_6$}.

RESULTS AND DISCUSSION

The $[M_2(B\text{-}\beta\text{-SiW}_8O_{31})_2]^{n-}$ clusters {M$_2$Si$_2$W$_{16}$} are all synthesized from the same set of reaction conditions. The procedure involves forming two solutions. Solution A comprises BHEP (2.5 g, 1.4 mmol) in 15 mL of deionized

water, acidified to pH 6.4 via addition of 4 M HCl or H₂SO₄. Solution B comprises K₈[γ-SiW₁₀O₃₆]·12H₂O (1.486 g, 0.5 mmol) and MCl₂·XH₂O (0.46 mmol) dissolved in 50 mL of 2 M NaCl. Solution A is added to solution B, and the pH is adjusted to 8.8. The resultant mixture is stirred for 20−30 min, depending on the transition metal used. The mixtures are then centrifuged and filtered into 50 mL conical flasks and left at 18 °C to crystallize. Crystals begin to form overnight, and are collected after one week. Average yields are 30−55% based on tungsten, with the exception being the nickel cluster, which only produces a few crystals and could not be optimized.

The architecture is a very simple sandwich structure comprising two {B-β-SiW₈} fragments coordinated to two transition metals. The central transition metals coordinate to the complete triads of the lacunary fragment and to an oxygen ligand coming from each silicon heteroatom (see Figure 1).
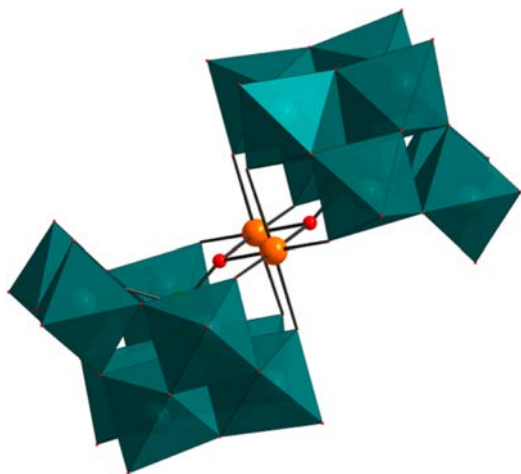

Figure 1. Polyhedral and ball-and-stick representation of {M₂(B-β-SiW₈O₃₁)₂} cluster. Color scheme: W = teal, M = orange, O = red.

The transition metals have no terminal water ligands, which is unusual for TMSPs. The architecture is very similar to the {M₃(H₂O)(B-β-XW₉O₃₄)(B-β-XW₈O₃₁)} unit found in several TMSPs;[12,25,28] however, it is missing one transition metal and one tungsten unit that completes the eclipsed triad of the {B-β-XW₉} fragment. Interestingly, the synthetic strategy employed to make the {M₂Si₂W₁₆} clusters is very similar to the method employed by Mitchell et al. that gave {Co₃(H₂O)(B-α/β-SiW₉O₃₄)(B-β-SiW₈O₃₁)},[29] and perhaps it can be postulated that the clusters we report here are intermediates in the formation of such clusters.

All of the compounds crystallize in the space group P$\overline{1}$ and with almost identical unit cell dimensions. This is unsurprising given that the only difference between the clusters is the transition metal present, and these metal centers are buried at the center of the cluster, not interacting with the sodium cations. The result of this is that the crystal packing is dependent only on the POM shell, which is identical across these clusters. The obvious exception is the {Fe₂Si₂W₁₆} cluster, which has a lower anionic charge and hence a smaller number of cations to pack around the same tungsten shell. The unit cell for the iron cluster is slightly smaller than that for the other compounds in the series

The solution behavior of the clusters was examined by ESI-MS; however, as sodium salts, there was very poor ionization from both aqueous and mixed aqueous−acetonitrile solutions.

To overcome this, cation exchange was performed, replacing sodium with tetrahexylammonium (THA) to give oily solids, which gave better ionization from acetonitrile solution. Such cationic exchange with bulky tetraalkylammonium cations to make POMs organic soluble is known.[30] Mass spectra were attainable for the copper-, cobalt-, and zinc-based clusters (see Figure 2 and Supporting Information). For {Cu₂Si₂W₁₆}, the
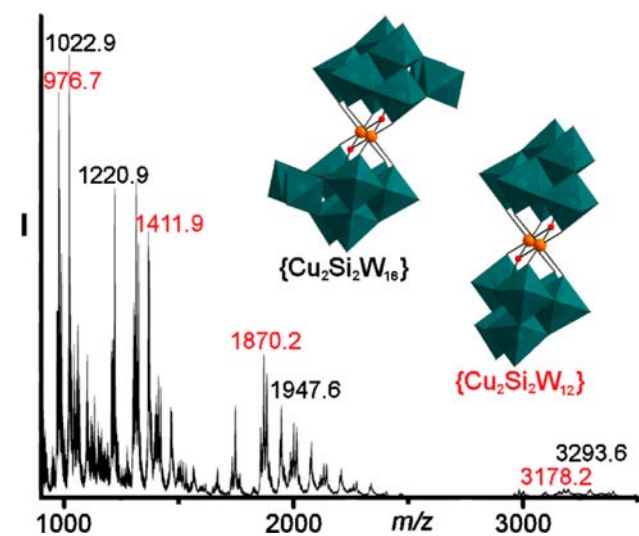

Figure 2. ESI-MS of THA[Cu₂(B-β-SiW₈O₃₁)₂] showing the most intense envelopes for the intact {Cu₂Si₂W₁₆} (highlighted in black) and fragmented {Cu₂Si₂W₁₂} species (highlighted in red).

intact parent cluster was observable at charge values of −2, −3, −4, and −5 at m/z 3293.6 {K₂Na₆(C₂₄H₅₂N)₆[Cu₂W₁₆Si₂O₆₂]·7H₂O}²⁻, 1947.6 {H₂Na₇(C₂₄H₅₂N)₄[Cu₂W₁₆Si₂O₆₂]·8H₂O}³⁻, 1220.9 {H₄K₂Na₅(C₂₄H₅₂N)[Cu₂W₁₆Si₂O₆₂]·12H₂O}⁴⁻, and 1022.9 {H₂Na₇(C₂₄H₅₂N)₂[Cu₂W₁₆Si₂O₆₂]·7H₂O}⁵⁻ (see Figure 2). This indicates that the cluster is stable enough to withstand the cation exchange process and the ionization conditions. Interestingly, there were envelopes assigned to {Cu₂Si₂W₁₂} species at −2, −3, −4, and −5 charge at m/z 3178.2 {H₅KNa₄(C₂₄H₅₂N)₈[Cu₂W₁₂Si₂O₅₂]·9H₂O}²⁻, 1870.2 {H₆K₂Na₃(C₂₄H₅₂N)₆[Cu₂W₁₂Si₂O₅₂]·6H₂O}³⁻, 1411.9 {H₄K₃Na₃(C₂₄H₅₂N)₆[Cu₂W₁₂Si₂O₅₂]·10H₂O}⁴⁻, and 976.7 {H₇Na₄(C₂₄H₅₂N)₄[Cu₂W₁₂Si₂O₅₂]·8H₂O}⁵⁻ (see Figure 2). The presence of such {Cu₂Si₂W₁₂} signals indicates that the cluster can decompose into a TMSP possessing smaller fragments. Around the main MS envelopes of each charge, described above, are several other less-intense signals. These envelopes also correspond to the intact {Cu₂Si₂W₁₆} cluster and {Cu₂Si₂W₁₂} fragment but possess different ratios of cations associated with the main POM anion—a common feature of ESI-MS of POMs. Full analysis of these envelopes can be found in the Supporting Information.

It is possible that the decomposition is occurring on just one of the Keggin fragments, but more probable is that each {β-SiW₈} is losing the two tungsten units that comprise the incomplete triad, to create a dimer of {SiW₆} units. This would keep the central {Cu₂} unit intact and retain its original coordination to the completed triads of the POM species. Whether the degradation of the {M₂Si₂W₁₆} cluster occurs in solution or in the mass spectrometer, the ESI-MS analysis implies a close relationship between the {β-SiW₈} and {SiW₆} clusters and that the most likely site for decomposition of the

$\{\beta\text{-SiW}_8\}$ is the incomplete triad. Similar envelopes for the $\{M_2Si_2W_{16}\}$ and $\{M_2Si_2W_{12}\}$ species could be identified for the cobalt and zinc clusters. (Full mass spectral analysis can be found in the Supporting Information.)

The $\{M_2Si_2W_{16}\}$ can be described as an open architecture because within the crystal structure the lacunary sites on the incomplete triad of the $\{\beta\text{-SiW}_8\}$ fragment are vacant, with not even sodium cations occupying the volume close to the central transition metals. In all other examples of TMSPs containing only $\{B\text{-}\beta\text{-SiW}_8\}$ fragments,[20−22,29,31] the lacunary sites of the tungsten POM are fully occupied, which means that the probability of them reacting further is limited. As the lacunary sites in the $\{M_2Si_2W_{16}\}$ cluster are vacant, it was hypothesized that these clusters could be used as starting materials in the synthesis of other, hopefully larger, TMSPs. The desire was to discover if these clusters could be used as reliable sources of $\{B\text{-}\beta\text{-SiW}_8\}$ fragments in other TMSPs and to observe what structural transformations, if any, could be achieved by lower nuclearity lacunary fragments.

Owing to the fact that the $\{M_2Si_2W_{16}\}$ architecture was available with several different transition metals, there was a large reaction space to explore. The decision was made to focus on homometallic systems first (i.e., reacting the $\{M_2Si_2W_{16}\}$ clusters with transition metal (TM) chloride salts such that M = TM) and based upon the findings to then try the more complex heterometallic systems. In the literature, the most abundant metals found coordinated to $\{B\text{-}\beta\text{-SiW}_8\}$ are Cu^{2+} and Co^{2+}. Cobalt has a tendency to form trimeric architectures with $\{SiW_8\}$,[22,29] whereas copper has shown the capacity to form dimers,[20] trimers,[31] and tetramers,[21] so initial experiments focused on copper.

The $\{Cu_2Si_2W_{16}\}$ was dissolved in water, and copper salts were introduced as solutions. Our preliminary experiments involved no external pH control other than that caused by varying the concentration of Cu^{2+} so as to allow the natural equilibria processes to be investigated. It was discovered that at high ratios of $\{Cu_2Si_2W_{16}\}/Cu^{2+}$ (1:<10) the cluster $Na_{16}[Cu_{14}(OH)_4(H_2O)_{16}(B\text{-}\beta\text{-SiW}_8O_{31})_4]\cdot20.5H_2O$ (Figure 3a) crystallized within two weeks. This is a tetramer of $\{B\text{-}\beta\text{-}$

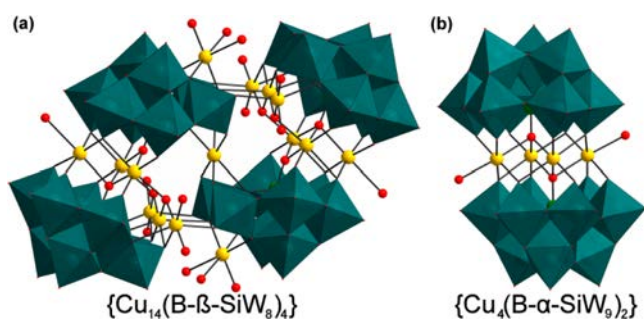**Figure 3.** Polyhedral and ball-and-stick representations of the two clusters formed by reacting $\{Cu_2Si_2W_{16}\}$ with $CuSO_4$ in water with no pH control.

$SiW_8\}$ fragments, previously reported by Zhang et al.[21] The formation of this cluster showed that the $\{M_2Si_2W_{16}\}$ clusters can be used as a source of $\{B\text{-}\beta\text{-SiW}_8\}$ in other TMSPs. The structure was confirmed by X-ray diffraction and Fourier transform infrared (FT-IR) analysis. The yield of this reaction was 42%, which is double that of the published procedure; however, the original synthesis directly uses $\{\gamma\text{-SiW}_{10}\}$, so when taking the initial preparation of $\{Cu_2Si_2W_{16}\}$ into consideration,

the yields are comparable. The literature procedure required the addition of D-proline, and similarly to the addition of BHEP in the synthesis of the $\{Cu_2Si_2W_{16}\}$ starting material, it is not fully understood what exact chemical influence it exerts. This provides further weight to the hypothesis that seemingly spectator organic cations can have significant influence over the reorganization of lacunary POMs.

When a lower ratio of $\{Cu_2Si_2W_{16}\}/Cu^{2+}$ is employed (1:5), the $\{Cu_{14}W_{32}\}$ cluster still forms within two weeks, albeit as a minor product. Yet, if this mother liquor is left longer, larger, pale blue/green crystals form after one month. These crystals are of the well-documented Weakley-sandwich architecture $[Cu_4(H_2O)_2(B\text{-}\alpha\text{-SiW}_9O_{36})_2]^{12-}$ (Figure 3b).[27] Formation of Weakley-sandwich clusters from TMSP reactions is common, but in this instance it was a surprise given that the starting material contains only $\{\beta\text{-W}_8\}$ units and that the Weakley sandwich contains $\{\alpha\text{-W}_9\}$ units. There is only one reported case of such a $\{\beta\text{-W}_8\}\text{-to-}\{\alpha\text{-W}_9\}$ transformation being observed, but this was within the mother liquor from a reaction that used sodium tungstate as a starting material.[32] In the absence of external tungstate, the increase in nuclearity shown within this system is not easy to explain. Examples of other POM fragments growing in nuclearity have been reported.[33]

For the lacunary fragments in this system to grow in size, some free tungstate must be present in solution. The only tungsten within the system is the $\{M_2Si_2W_{16}\}$ precursor itself, which strongly implies that a level of decomposition of the starting material occurs during the reaction. The most likely site for decomposition is the monovacant eclipsed triad on the $\{B\text{-}\beta\text{-SiW}_8\}$ units, as it is not coordinated to the metal centers. Decomposition at this site would be analogous to the manner in which it is proposed $\{\gamma\text{-SiW}_{10}O_{36}\}$ initiates its reorganization.[19] Such decomposition would result in the formation of $\{SiW_6\}$ lacunae. Given this postulation, there would now be free tungstate in solution, and it has been shown that free tungstate, in the absence of heteroatoms, can form $\{W_3O_{10}\}$ Keggin triad-like units.[34] It is conceivable that such $\{W_3O_{10}\}$ units could recombine with the $\{SiW_6\}$ fragment in such a manner that $\{B\text{-}\alpha\text{-SiW}_9\}$ fragments could form. (It is worth noting that the most common partner for $\{SiW_6\}$ fragments in TMSPs is $\{B\text{-}\alpha\text{-SiW}_9\}$, which implies that there is a strong link between these two species.)[23,35] A decomposition−reconstitution mechanism appears the most feasible for explaining both the increase in nuclearity and the change in Keggin isomeric form (see Scheme 1). Via this strategy, the formation of $\{B\text{-}\beta\text{-SiW}_9\}$ would also be possible.

As stated above, the ESI-MS analysis of the parent $\{Cu_2Si_2W_{16}\}$ cluster showed envelopes corresponding to a fragmented $\{Cu_2(SiW_6)_2\}$ species. This would support the hypothesized decomposition−reconstitution mechanism for the reorganization of $\{\beta\text{-SiW}_8\}$, as the fragmented $\{SiW_6\}$ units are still coordinated to the central copper ions, and the loss in tungsten could only come from decomposition of the incomplete triads. In the synthesis of the Weakley sandwich cluster from $\{Cu_2Si_2W_{16}\}$, based upon the observations made via MS, it is possible to suggest that during the entire transformation, the central two Cu ions remain coordinated to the POM. Hence, this strategy could be used as a route toward the fabrication of mixed TMSPs, by selecting one transition metal in the starting material and introducing a second in solution. With improvements made to the ionization of species in water, it may be possible to follow the POM transformation

Scheme 1. Proposed Mechanism for the Transformation of {B-β-SiW$_8$} into {B-α-SiW$_9$} in the Absence of Any External Source of Tungstate
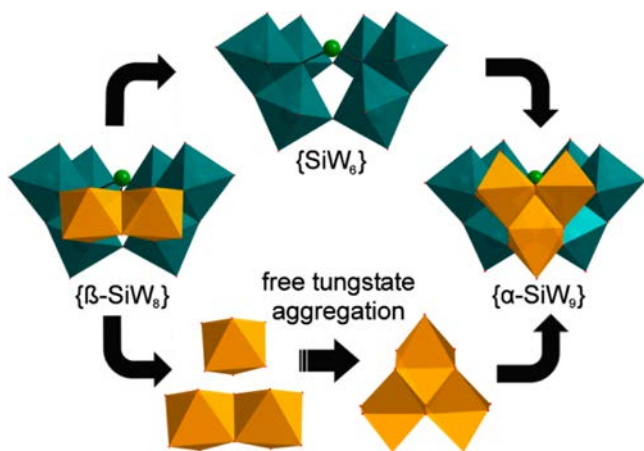
directly via ESI-MS and further our understanding of how low-nuclearity POMs transform into one another.

EXPERIMENTAL SECTION

K$_8$[γ-SiW$_{10}$O$_{36}$]·12H$_2$O was prepared according to the literature procedure.[36] Purity was confirmed by IR analysis. All other chemicals were purchased from SigmaAldrich and used without further purification.

1. Synthesis of [M$_2$(B-β-SiW$_8$O$_{31}$)$_2$]$^{n-}$ Clusters. *1.1. Synthesis of Na$_{15}$H[{Co^{II}SiW$_8$O$_{31}$}$_2$]·49H$_2$O.* BHEP (2.5 g, 1.4 mmol) was dissolved to give a colorless solution (A). The pH of solution A was adjusted to 8.64 using 2 M H$_2$SO$_4$. In 50 mL of 2 M NaCl solution was dissolved K$_8$[γ-SiW$_{10}$O$_{36}$]·12H$_2$O (1.49 g, 0.5 mmol) and CoCl$_2$·6H$_2$O (0.110 g, 0.46 mmol), to give a pink/red solution (B). Solution A was added to solution B to give a pink solution, which was adjusted to pH 8.80 via addition of 2 M H$_2$SO$_4$ dropwise. The resultant solution was stirred for 30 min. After this time the pH was typically 8.7. The solution was filtered into a wide-necked 100 mL conical flask and left in a temperature-controlled environment at 18 °C to crystallize via slow evaporation. Pink needle-shaped crystals obtained overnight. Yield = 0.421 g, 0.079 mmol (31.6% based on W). Characteristic FT-IR (powder) bands (cm^{-1}): 3383 (b), 1638 (b), 1125 (m), 970 (m), 930 (sh), 855 (sh), 816 (s), 688 (b), 6.8 (w). UV band: λ = 554 nm, ε = 71 M^{-1} cm^{-1}. Elemental analysis: Co$_2$H$_{99}$Na$_{15}$O$_{111}$Si$_2$W$_{16}$, MW = 5336.28 g mol^{-1}. Anal. Calcd (%): W (55.1), Co (2.21), Na (6.46); found: W (52.4), Co (2.57), Na (6.01). Thermogravimetric analysis (TGA) water loss over 25−450 °C for partially dehydrated sample Co$_2$H$_{77}$Na$_{15}$O$_{100}$Si$_2$W$_{16}$ (%); calculated: 13.3; found: 13.1.

1.2. Synthesis of Na$_{15}$H[{Mn^{II}SiW$_8$O$_{31}$}$_2$]·49H$_2$O. Same method as above, but using MnCl$_2$ (anhydrous beads, 0.057 g, 0.46 mmol). Yellow needle shaped crystals obtained overnight. Yield = 0.497 g, 0.093 mmol (37.2% based on W). Characteristic FT-IR (powder) bands (cm^{-1}): 3383 (b), 1640 (b), 1125 (m), 972 (m), 930 (sh), 852 (sh), 808 (sh), 700 (b), 606 (w). UV band: λ = 388 nm, ε = 115 M^{-1} cm^{-1}. Elemental analysis: H$_{99}$Mn$_2$Na$_{15}$O$_{111}$Si$_2$W$_{16}$, MW = 5328.30 g mol^{-1}. Anal. Calcd (%): W (55.2), Mn (2.06), Na (6.47); found: W (51.1), Mn (2.33), Na (5.90). TGA water loss over 25−450 °C for partially dehydrated sample H$_{77}$Mn$_2$Na$_{15}$O$_{100}$Si$_2$W$_{16}$ (%); calculated: 13.3; found: 13.3.

1.3. Synthesis of Na$_{15}$H[{Ni^{II}SiW$_8$O$_{31}$}$_2$]·49H$_2$O. Same method as above, but using NiCl$_2$·6H$_2$O (0.109 g, 0.46 mmol). Small green block shaped crystals (3−4) obtained overnight. Insufficient material to measure a yield or any further physical characteristics. Formula determined from crystallography alone to give MW = 5335.84 g mol^{-1}.

1.4. Synthesis of Na$_{15}$H[{Zn^{II}SiW$_8$O$_{31}$}$_2$]·49H$_2$O. Same method as above, but using ZnCl$_2$ (0.063 g, 0.46 mmol). Colorless crystals obtained overnight. Yield = 0.776 g, 0.145 mmol (58.0% based on W).

Characteristic FT-IR (powder) bands (cm^{-1}): 3381 (b), 1632 (b), 1125 (m), 970 (w), 932 (sh), 853 (sh), 822 (s), 688 (b), 619 (w). Elemental analysis: H$_{99}$Na$_{15}$O$_{111}$Si$_2$W$_{16}$Cu$_2$, MW = 5349.16 g mol^{-1}. Anal. Calcd (%): W (55.0), Zn (2.44), Na (6.45); found: W (49.8), Zn (2.93), Na (6.41). TGA water loss over 25−450 °C for partially dehydrated H$_{77}$Na$_{15}$O$_{100}$Si$_2$W$_{16}$Cu$_2$ (%); calculated: 13.3; found: 13.1.

1.5. Synthesis of Na$_{15}$H[{Cu^{II}SiW$_8$O$_{31}$}$_2$]·49H$_2$O. Same method as above, but using CuCl$_2$·2H$_2$O (0.079 g, 0.46 mmol). Pale blue-green crystals appeared overnight. Yield = 0.487 g, 0.091 mmol (36.4% based on W). Characteristic FT-IR (powder) bands (cm^{-1}): 3358 (b), 1626 (b), 1098 (w), 970 (w), 932 (sh), 841 (s), 692 (b), 637 (w), 617 (w). UV band: λ = 798 nm, ε = 40.0 M^{-1} cm^{-1}. Elemental analysis: H$_{99}$Na$_{15}$O$_{111}$Si$_2$W$_{16}$Cu$_2$, MW = 5345.5 g mol^{-1}. Anal. Calcd (%): W (55.0), Cu (2.37), Na (6.45); found: W (55.5), Cu (2.67), Na (6.07). TGA water loss over 25−450 °C for partially dehydrated H$_{67}$Na$_{15}$O$_{95}$Si$_2$W$_{16}$Cu$_2$ (%); calculated: 11.7; found: 11.5.

1.6. Synthesis of Na$_{13}$H[{Fe^{III}SiW$_8$O$_{31}$}$_2$]·42H$_2$O. Same method as above, but using FeCl$_2$·4H$_2$O (0.091 g, 0.46 mmol). The solution is initially brown but turns yellow overnight. Dark yellow crystals form overnight. Yield = 0.630 g, 0.121 mmol (48.8% based on W). Characteristic FT-IR (powder) bands (cm^{-1}): 3335 (b), 1630 (b), 1125 (m), 977 (sh), 930 (sh), 847 (s), 808 (sh), 791 (w), 711 (b), 650 (w), 630 (w), 619 (w). UV band: λ = 458 nm, ε = 13.8 M^{-1} cm^{-1}. Elemental analysis: H$_{85}$Fe$_2$Na$_{13}$O$_{104}$Si$_2$W$_{16}$, MW = 5158.0 g mol^{-1}. Anal. Calcd (%): W (57.0), Fe (2.17), Na (5.79); found: W (55.3), Fe (2.76), Na (6.14). TGA water loss over 25−450 °C for partially dehydrated sample H$_{47}$Fe$_2$Na$_{13}$O$_{85}$Si$_2$W$_{16}$ (%); calculated: 8.6; found: 8.5.

2. Formation of Tetrahexylammonium Salts of {M$_2$(B-β-SiW$_8$O$_{31}$)} Clusters for ESI-MS. To 50 mg of {M$_2$(B-β-SiW$_8$O$_{31}$)$_2$} sodium salt, dissolved in 3 mL of deionized water in a test tube was added 100 mg of tetrahexylammonium bromide. An oily residue began to form, and the mixture was left overnight. This residue sank to the bottom. The solvent was decanted off, and the residue was dissolved in 3 mL of MeCN. The residue was reprecipitated by addition of 5 mL of H$_2$O, and the solvent was decanted. The reprecipitation was performed a total of three times, and then the oily residue was used directly in ESI-MS experimentation without purification.

3. Use of Na$_{15}$H[{Cu^{II}SiW$_8$O$_{31}$}$_2$]·49H$_2$O as a Starting Material. *3.1. Synthesis of Na$_{16}$[Cu$_{14}$(OH)$_4$(H$_2$O)$_{16}$(SiW$_8$O$_{31}$)$_4$]·20.5H$_2$O.* To a solution of Na$_{15}$H[{Cu^{II}SiW$_8$O$_{31}$}$_2$]·49H$_2$O (0.100 g, 1.87 × 10^{-2} mmol) in 5 mL of H$_2$O, with stirring in a 14 mL vial was added 300 μL of 1 M CuSO$_4$·5H$_2$O. The resultant blue solution was stirred for 1 h, and then the pH was measured as 3.6. The solution was left directly to crystallize in a temperature-controlled room at 18 °C, without filtering first. After one week blue-green block crystals of the product were visible, but the crystals were not collected until after one month. Yield = 42 mg, 4.2 × 10^{-3} mmol (45% based on W). The compound was confirmed as the published Na$_{16}$[Cu$_{14}$(OH)$_4$(H$_2$O)$_{16}$(SiW$_8$O$_{31}$)$_4$]·20.5H$_2$O[21] compound via unit cell checking and IR analysis.

3.2. Synthesis of Na$_{12}$[Cu$_4$(H$_2$O)$_2$(SiW$_9$O$_{34}$)$_2$]·39H$_2$O. To a solution of Na$_{15}$H[{Cu^{II}SiW$_8$O$_{31}$}$_2$]·49H$_2$O (0.200 g, 3.74 × 10^{-2} mmol) in 10 mL of H$_2$O, with stirring in a 14 mL vial was added 90 μL of 1 M CuSO$_4$·5H$_2$O and 30 μL of H$_2$O. The resultant blue solution was stirred for 1 h, and then the pH was measured as 6.6. The solution was left directly to crystallize in a temperature-controlled room at 18 °C, without filtering first. After two months <10 mg of Na$_{15}$H[{Cu^{II}SiW$_8$O$_{31}$}$_2$]·49H$_2$O formed. The mother liquor was left to crystallize for longer, and when the solution was nearing dryness, larger pale blue-green crystals formed. Yield = 93 mg, 1.63 × 10^{-2} mmol (48.9% based on W). Characteristic FT-IR (powder) bands (cm^{-1}): 3315 (b), 1629 (s) 1135 (w), 1099 (w), 985 (w), 939 (sh), 860 (sh), 846 (sh), 705 (s), 678 (w), 666 (w), 609 (w). UV band: λ = 757 nm, ε = 116 M^{-1} cm^{-1}. Elemental analysis: H$_{82}$Cu$_4$Na$_{12}$O$_{109}$Si$_2$W$_{18}$, MW = 5722.2 g mol^{-1}. Anal. Calcd (%): W (57.8), Cu (4.44), Na (4.82); found: W (58.0), Cu (5.5), Na (4.52). TGA water loss over 25−450 °C for partially dehydrated sample calculated H$_{64}$Cu$_4$Na$_{12}$O$_{100}$Si$_2$W$_{18}$ (%); calculated: 9.7; found: 9.8.

CONCLUSIONS

We have reported the facile synthesis of a series of $\{B\text{-}\beta\text{-}SiW_8O_{31}\}$-based TMSP dimers that can be synthesized with many different first-row transition metals. The reaction makes use of BHEP organic base to buffer the reaction. ESI-MS of $\{Cu_2Si_2W_{16}\}$ showed that the cluster is stable but can readily fragment into smaller $\{SiW_6\}$-containing dimers. The $\{Cu_2Si_2W_{16}\}$ was successfully shown to be a precursor for the synthesis of other TMSPs, one of which was the Weakley sandwich cluster $\{Cu_4(H_2O)(B\text{-}\alpha\text{-}SiW_9O_{34})_2\}$. The formation of the Weakley sandwich represents the first reported observation of a direct lacunary Keggin transformation from $\{B\text{-}\beta\text{-}SiW_8\}$ in the absence of an external source of tungstate, showing that small lacunary POMs can still undergo significant structural reorganization. We proposed the transformation occurs as follows: (1) Free tungstate was generated by an initial decomposition to $\{SiW_6\}$. (2) The free tungstate assembles into $\{W_3\}$ units. (3) The $\{SiW_6\}$ recombines with the $\{W_3\}$ unit to form the final $\{B\text{-}\alpha\text{-}SiW_9\}$ species. It is still unclear whether the central copper atoms remain coordinated to the POM throughout the process. These $\{M_2Si_2W_{16}\}$ structures have significant potential as starting materials for homo- and heterometallic TMSPs and with continued study could provide greater insight into the mechanisms behind the structural transformations accessible by Keggin lacunae.

ASSOCIATED CONTENT

ⓈSupporting Information

Full syntheses, ESI-MS experimentation and spectra, tabulated m/z data, THA salt analysis, crystallographic methods and equations, single-crystal X-ray data, and additional references. This material is available free of charge via the Internet at http://pubs.acs.org.

AUTHOR INFORMATION

Corresponding Author

*E-mail: lee.cronin@glasgow.ac.uk.

Notes

The authors declare no competing financial interest.

ACKNOWLEDGMENTS

REFERENCES

(1) Mizuno, N.; Misono, M. *J. Mol. Catal.* **1994**, *86*, 319.
(2) Kamata, K.; Yonehara, K.; Sumida, Y.; Yamaguchi, K.; Hikichi, S.; Mizuno, N. *Science* **2003**, *300*, 964.
(3) Proust, A.; Matt, B.; Villanneau, R.; Guillemot, G.; Gouzerh, P.; Izzet, G. *Chem. Soc. Rev.* **2012**, *41*, 7605.
(4) Long, D.-L.; Burkholder, E.; Cronin, L. *Chem. Soc. Rev.* **2007**, *36*, 105.
(5) Clemente-Juan, J. M.; Coronado, E.; Gaita-Arino, A. *Chem. Soc. Rev.* **2012**, *41*, 7464.
(6) Zheng, S.-T.; Yang, G.-Y. *Chem. Soc. Rev.* **2012**, *41*, 7623.
(7) Yamase, T. *J. Mater. Chem.* **2005**, *15*, 4773.
(8) Mitchell, S. G.; Streb, C.; Miras, H. N.; Boyd, T.; Long, D.-L.; Cronin, L. *Nature Chem.* **2010**, *2*, 308.
(9) Fang, X.; Kögerler, P. *Angew. Chem., Int. Ed.* **2008**, *47*, 8123.
(10) Bassil, B. S.; Ibrahim, M.; Al-Oweini, R.; Asano, M.; Wang, Z.; van Tol, J.; Dalal, N. S.; Choi, K.-Y.; Ngo Biboum, R.; Keita, B.; Nadjo, L.; Kortz, U. *Angew. Chem., Int. Ed.* **2011**, *50*, 5961.
(11) Contant, R.; Hervé, G. *Rev. Inorg. Chem.* **2002**, *22*, 63.
(12) Chen, L.; Shi, D.; Zhao, J.; Wang, Y.; Ma, P.; Wang, J.; Niu, J. *Cryst. Growth Des.* **2011**, *11*, 1913.
(13) Bassil, B. S.; Kortz, U. *Dalton Trans.* **2011**, *40*, 9649.
(14) Assran, A. S.; Mal, S. S.; Izarova, N. V.; Banerjee, A.; Suchopar, A.; Sadakane, M.; Kortz, U. *Dalton Trans.* **2011**, *40*, 2920.
(15) Botar, B.; Kögerler, P. *Dalton Trans.* **2008**, 3150.
(16) Kortz, U.; Matta, S. *Inorg. Chem.* **2001**, *40*, 815.
(17) Zhang, Z.; Li, Y.; Wang, E.; Wang, X.; Qin, C.; An, H. *Inorg. Chem.* **2006**, *45*, 4313.
(18) Zhang, Z.; Li, Y.; Chen, W.; Wang, E.; Wang, X. *Inorg. Chem. Commun.* **2008**, *11*, 879.
(19) Winter, R. S.; Cameron, J. M.; Cronin, L. *J. Am. Chem. Soc.* **2014**, *136*, 12753.
(20) Luo, Z.; Kögerler, P.; Cao, R.; Hakim, I.; Hill, C. L. *Dalton Trans.* **2008**, 54.
(21) Zhang, Z.; Qi, Y.; Qin, C.; Li, Y.; Wang, E.; Wang, X.; Su, Z.; Xu, L. *Inorg. Chem.* **2007**, *46*, 8162.
(22) Bassil, B. S.; Nellutla, S.; Kortz, U.; Stowe, A. C.; van Tol, J.; Dalal, N. S.; Keita, B.; Nadjo, L. *Inorg. Chem.* **2005**, *44*, 2659.
(23) Mitchell, S. G.; Miras, H. N.; Long, D.-L.; Cronin, L. *Inorg. Chim. Acta* **2010**, *363*, 4240.
(24) Mitchell, S. G.; Molina, P. I.; Khanra, S.; Miras, H. N.; Prescimone, A.; Cooper, G. J. T.; Winter, R. S.; Brechin, E. K.; Long, D.-L.; Cogdell, R. J.; Cronin, L. *Angew. Chem., Int. Ed.* **2011**, *50*, 9154.
(25) Bassil, B. S.; Kortz, U.; Tigan, A. S.; Clemente-Juan, J. M.; Keita, B.; de Oliveira, P.; Nadjo, L. *Inorg. Chem.* **2005**, *44*, 9360.
(26) Lisnard, L.; Mialane, P.; Dolbecq, A.; Marrot, J.; Clemente-Juan, J. M.; Coronado, E.; Keita, B.; de Oliveira, P.; Nadjo, L.; Sécheresse, F. *Chem.—Eur. J.* **2007**, *13*, 3525.
(27) Weakley, T. J. R.; Finke, R. G. *Inorg. Chem.* **1990**, *29*, 1235.
(28) Chu, L.; Zhou, B.; Wang, C.; Zhao, Z.; Su, Z.; Yu, K. *Solid State Sci.* **2011**, *13*, 488.
(29) Mitchell, S. G.; Ritchie, C.; Long, D.-L.; Cronin, L. *Dalton Trans.* **2008**, 1415.
(30) Herrman, S.; Kostrzewa, M.; Wierschem, A.; Streb, C. *Angew. Chem., Int. Ed.* **2014**, *53*, 13596.
(31) Mialane, P.; Dolbecq, A.; Marrot, J.; Rivière, E.; Sécheresse, F. *Chem.—Eur. J.* **2005**, *11*, 1771.
(32) Yang, L.; Ma, X.; Ma, P.; Hua, J.; Niu, J. *Cryst. Growth Des.* **2013**, *13*, 2982.
(33) Khoshnavazi, R.; Naseri, E.; Tayamon, S.; Moaser, A. G. *Polyhedron* **2011**, *30*, 381.
(34) Vilà-Nadal, L.; Rodríguez-Fortea, A.; Yan, L.-K.; Wilson, E. F.; Cronin, L.; Poblet, J. M. *Angew. Chem., Int. Ed.* **2009**, *48*, 5452.
(35) Zhang, Z.; Wang, E.; Chen, W.; Tan, H. *Aust. J. Chem.* **2007**, *60*, 284.
(36) Canny, J.; Tézé, A.; Thouvenot, R.; Hervé, G. *Inorg. Chem.* **1986**, *25*, 2114.

NOTE ADDED AFTER ASAP PUBLICATION

This paper was published on the Web on April 7, 2015, with minor errors in level heading 1.5. The corrected version was reposted on April 20, 2015.